ADVANCED SCIENCE NEWS
www.advancedsciencenews.com

Fullerene-Like Nickel Oxysulfide Hollow Nanospheres as Bifunctional Electrocatalysts for Water Splitting

*Junli Liu, Yong Yang, Bing Ni, Haoyi Li, and Xun Wang**

With the increasing demands of energy and consumption of fossil fuel, it has become a prevailing trend to explore new methods used for efficient extraction of energy. Recently, electrochemical water splitting has attracted tremendous attention to produce eco-friendly, renewable, and clean hydrogen and oxygen energy.[1] In order to increase the reaction rate and lower the overpotential,[2] it is necessary to develop highly efficient electrocatalysts for HER (hydrogen evolution reaction) and OER (oxygen evolution reaction).[3] Pt-group metals are currently the state-of-the-art catalysts for HER[4] and Ir-, Ru-based materials show the highest OER activity.[5] Nevertheless, the scarce, high cost, low bifunctionality shortcomings of these kinds of noble metal catalysts limit their applications.[6] Recently, non-noble metal (e.g., Ni, Co, Fe, Mo, and W)-based materials have been explored extensively as HER or OER electrocatalysts on various supports.[7] And there is no doubt that non-noble metal chalcogenides among these materials have attracted considerable research interests in studying their excellent electrochemical properties as catalysts for HER or OER.[8] For example, Xu et al. reported ultrasmall Cu_7S_4@MoS_2 heteronanoframes with abundant active edge sites for ultrahigh-performance hydrogen evolution.[9] Lin et al. reported a Ni_3S_2 and multiwalled carbon nanotubes nanocomposite with high catalytic activity for HER.[10] Zhou et al. synthesized Ni_3S_2 nanorods as an efficient electrocatalyst for OER.[11] Consequently, it is important to design advanced electrocatalysts for HER and OER by tuning the structure of non-noble metal chalcogenides. However, there still are some difficulties for sulfides in electrocatalytic performance, such as the difficulty of preparation and poor stability. Moreover, some sulfides could not catalyze the HER and OER simultaneously and during the electrochemically catalytic process, they usually perform poor stability and change into oxides or hydroxides.[12]

In this work, we successfully prepared a sort of fullerene-like nickel oxysulfide bifunctional electrocatalyst by a solvothermal method. We found the fullerene-like nickel oxysulfide hollow nanospheres (FNHNs) with little HER and OER activity by itself. However, when constructed by in situ growth on the surface of nickel foam, such fullerene-like nickel oxysulfide hollow nanospheres/Ni foam composite (FNHNs/NF) exhibited exhilaratingly high HER and OER performance simultaneously in 1 M KOH, which could be attributed to the synergetic effect of the proper ratios of sulfur and oxygen. We predict this work could open up a very promising prospect for non-noble metal oxysulfides as bifunctional electrocatalysts.

In a typical synthesis, by taking advantage of sulfur powder and nickel chloride hexahydrate as precursors and *n*-octylamine, oleic acid, and ethanol as solvents, FNHNs were facilely obtained at 180 °C for 8 h (details in the Supporting Information). The FNHNs/NF was synthesized just by adding a piece of clean nickel foam (≈1 × 2 cm^2) to above FNHNs system, and after 8 h at 180 °C we successfully obtained the composite (details in the Supporting Information). **Figure 1**a,b displays transmission electron microscopy (TEM) images with different magnifications, and Figure 1c,d shows the high angle annular dark field scanning transmission electron microscopy (HAADF-STEM) images of FNHNs. The closed cage structures shown in TEM and the 3D round shapes shown in STEM images demonstrate that we really prepared fullerene-like hollow nanospheres with diameters about 40–50 nm and interlayer spacing about 3 nm. The TEM image of FNHNs detached ultrasonically from the Ni foam substrate is displayed in Figure S1 (Supporting Information). Figure S2a,b (Supporting Information) shows scanning electron microscopy (SEM) patterns of FNHNs and FNHNs/NF, respectively. Interestingly, the morphology of fullerene-like hollow nanospheres has almost not changed after being decorated on the surface of nickel foam. Furthermore, as the best of our knowledge, the nickel foam possesses electrocatalytic property due to the special porous structure, which could provide extensive surface to connect with FNHNs. As a consequence, the synergetic effect of FNHNs and nickel foam makes it favor the transmission of gas and electrolyte in improving its electrocatalytic performance.[5] To identify the component of FNHNs, a series of characterizations including the energy dispersive spectroscopy line scan, X-ray diffraction (XRD), X-ray photoelectron spectra (XPS), and inductively coupled plasma optical emission spectrometer (ICP-OES) were performed. The energy dispersive spectroscopy line scan of FNHNs (Figure 1g) displays the composition difference in outer and inner nanospheres. Indeed, the dispersion of constituents confirms we obtain the fullerene-like nickel oxysulfide hollow nanospheres. XRD (Figure S3a,b,

J. Liu, Dr. Y. Yang, B. Ni, H. Li, Prof. X. Wang
Key Lab of Organic Optoelectronics
and Molecular Engineering
Department of Chemistry
Tsinghua University
Beijing 100084, China
E-mail: wangxun@mail.tsinghua.edu.cn

DOI: 10.1002/smll.201602637

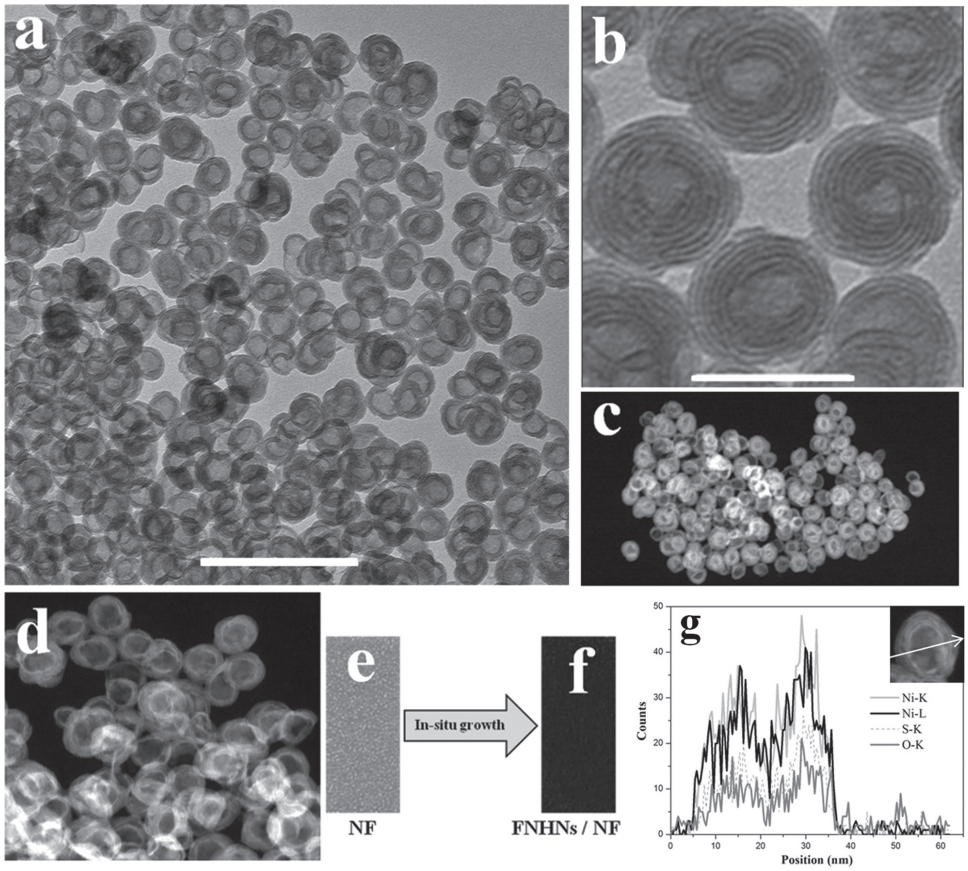

Figure 1. a,b) TEM images of FNHNs with different magnifications. c,d) STEM images of FNHNs. e) Bare Ni foam substrate. f) In situ growth of FNHNs on Ni foam. g) Energy dispersive spectroscopy line scan of FNHNs suggests composition difference in outer and inner nanospheres, in which the red arrow (inset) shows the scan direction. Scale bar: a) 200 nm; b) 50 nm.

Supporting Information) and ICP-OES (Table S1, Supporting Information) data suggest the products are mixture of nickel sulfide and nickel oxide, which is consistent with XPS data (Figure S4a,b, Supporting Information). The fitted peaks of Ni at 875.1 eV ($2p_{1/2}$) and 857.3 eV ($2p_{3/2}$), S at 168.6 eV ($2p_{1/2}$) and 161.7 eV ($2p_{3/2}$) are similar to those reported for Ni_3S_2, NiS, NiS_2, and NiO.[1b,15] And the corresponding formula of the oxysulfide was given of $NiS_{0.28}O_{0.72}$.

We also continue to carry out a series of experiments to investigate the mechanism. We found the ratios of sulfur and ethanol are not the crucial factors for the formation of FNHNs, and they just could influence the purity (Figures S5 and S6, Supporting Information). Nevertheless, temperature and reaction time could affect the morphology directly. A series of TEM images suggest the FNHNs are difficult to form at low temperature (Figure S7a, Supporting Information). And when temperature is set higher, although FNHNs exist, there also appear some sheets and tubes (Figure S7b,c, Supporting Information). Furthermore, we also investigate the formation process of FNHNs at different reaction time (Figure S8, Supporting Information). Interestingly, there are just some nanoparticles before 3 h, but from 3 h, there start appearing plenty of FNHNs and multiwalled nanotubes (MWNs) (Figure S8c, Supporting Information). Consequently, we consider the nanoparticles assembly into MWNs, which self-roll to form the FNHNs. With the reaction time extending, nearly all MWNs transfer into FNHNs, and there are no MWNs being observed. In other words, after 3 h, reaction time just could impact the purity of materials (Figure S8d,e, Supporting Information). Of course, the transformation between MWNs and FNHNs is a reversible procedure. At higher temperature, FNHNs also could dissociate into MWNs (Figure S7c, Supporting Information). At the same time, hetero metal ions have been also studied (Figures S9–S11, Supporting Information). Although the composition changes (Figure S3c, Supporting Information), the morphology of FNHNs is still kept. Moreover, the FNHNs possess layer-by-layer structure. **Figure 2**a exhibits the result of small angle X-ray diffraction (SAXD) of FNHNs. Obviously, there appears an evident peak at 2.86°(2θ), which corresponds to layer spacing of 3.09 nm according to Bragg equation. Thermo gravimetric analysis (TGA) and differential thermal analysis (DTA) were used to test the amount of residual organic component in FNHNs. Figure 2b displays the TGA (black line) and DTA (red line) curves, which indicate a gradual slope before 300 °C resulting from the decomposition of *n*-octylamine and oleic acid, and the mass is about 3.5%. After 300 °C, the sharp decline could be attributed to the collapse of fullerene-like hollow nanospheres structure and the decomposition of nickel oxysulfide, and during the process, there also follows a relatively evident endothermic peak at ≈500 °C (DTA curve).

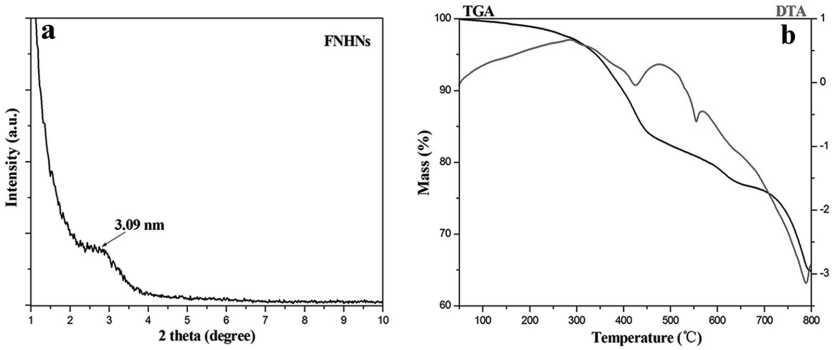

Figure 2. a) Small angle X-ray diffraction (SAXD) of FNHNs. b) TGA and DTA curves of FNHNs. The data were collected under argon gas atmosphere with a temperature increasing rate of 10 °C min^{-1}.

The nickel foam acts as a substrate that anchors the FNHNs. And the resulting nickel foam surface is completely black in color (Figure 1e,f), indicating the uniform formation of FNHNs on the surface of nickel foam. Then the electrocatalytic OER activity of the FNHNs/NF (**Figure 3**) was tested in an alkaline solution (1 M KOH) using a standard three-electrode system (without iR compensation). As comparison, FNHNs, $CoNi_2S_4$, and Ni foam were also measured under identical conditions. The linear sweep voltammetry (LSV) (Figure 3a) and cyclic voltammetry (CV) (Figure S12, Supporting Information) curves exhibit significant differences in OER activities of different materials. All potentials were measured against a saturated calomel electrode and are reported with respect to a reversible hydrogen electrode (RHE). All the current density for nickel foam based materials represented the geometric current density, because it was difficult to measure the true area of nickel foam. Obviously, the FNHNs/NF perform excellent OER activity, which exhibit a low overpotential of 0.29 V at the current density of 10 mA cm^{-2} and a Tafel slope of 62.38 mV dec^{-1} (Figure 3b). At the same condition, the FNHNs just possess little OER performance, which could be attributed to the diameter of FNHNs (≈50 nm). It is reasonable to consider that electrons are difficult to transfer between different FNHNs, while the introduction of nickel foam could improve the conductivity as well as the activity of FNHNs. According to related report, electrochemical surface area and conductivity are two vital factors, which could increase the activity of catalysts.[13] Accordingly, the electrochemically active surface area was estimated from the electrochemical double layer capacitance. And CV was carried out to investigate the electrochemical double layer capacitance at non-Faradaic overpotentials (Figure S13, Supporting Information). Obviously, the result suggested that FNHNs/NF really provide larger active area than NF for more catalytic reactions to occur on it. As far as we know, the nickel foam is a kind of polyporous material and own fine electrochemical performance (Figure 3a,b) to some degree. Additionally, maybe during the process of the in situ directional growth of FNHNs on the nickel foam, oleic acid and *n*-octylamine as ligands were removed from the surface of spheres, which dramatically improve the conductivity and expose the catalytic surface. And we also investigated the change of FNHNs/NF before and after OER by means of XPS (Figure S14, Supporting Information). It revealed that after OER the peak of metal nickel disappeared and the amount of oxygen increased evidently. This result suggested there was the oxide layer forming on the surface of nickel based material, which also could improve the catalytic performance for OER.[14] Moreover, we also measured the $CoNi_2S_4$ FNHNs (preparation and characterization seen in Figures S3b and S4c–e, Supporting Information). It requires an overpotential of 0.34 V to afford a current density of 10 mA cm^{-2} and Tafel slope of 68.76 mV dec^{-1} (Figure 3a,b), which performs higher catalytic activity than nickel foam and nickel oxysulfide nanospheres. To the best of our knowledge, some derivatives of cobalt also possess favorable electrocatalytic property.[15] So it is reasonable to explain that the introduction of cobalt salt could further ameliorate the property in electrochemical catalyst. In addition to the catalytic activity, we also investigated the long term electrochemical stability of the FNHNs/NF (Figure 3c) for OER at a static potential of 1.578 V versus RHE. The stability line reveals that after 10 h, the current density increased. XPS was adopted to investigate the FNHNs/NF before and after OER stability test (Figure S14, Supporting Information). The result implied that maybe there was an oxide layer forming on the surface of material,[6,16] which could ameliorate the performance of OER[17] and lead to the current density increasing.

To probe the fitness of FNHNs/NF catalysts in the full water splitting process, we also did the HER performance test of all samples in 1 M KOH solution in a three-electrode system. **Figure 4**a,b shows the results of LSV and Tafel slope. For the FNHNs/NF, onset potential is ≈–50 mV (vs RHE) and an overpotential of 0.14 V was needed to reach the current density of 10 mA cm^{-2} with a Tafel slope of 81.63 mV dec^{-1}. Such a Tafel slope of the FNHNs/NF suggests a combined Volmer–Heyrovsky mechanism for hydrogen evolution. And the excellent HER performance could be ascribed to the removal of ligands from FNHNs, which gives rise to the improvement of conductivity and catalytic surface exposed. Furthermore, the special porous structure of nickel foam could offer large electrochemical surface and result in more active site exposed. Accordingly, the FNHNs/NF HER activity (onset potential ≈–50 mV) nearly competes with Pt/C (20%) (onset potential 0 V). Meanwhile the result also reveals that artful construction can directly influence catalytic activity. Although the onset potentials of nickel oxysulfide and $CoNi_2S_4$ (corresponding to 0.295 and 0.2 V, respectively) are higher than FNHNs/NF. At least, to some extent, it indicates that the introduction of cobalt could increase the amount of active sites and improve the HER performance (Figure S15, Supporting Information). The durability test of FNHNs/NF (Figure 4c) was operated at the static potential of –0.242 V for 10 h. The XPS peak of nickel (Figure S14, Supporting Information) showed the metal nickel peak disappeared after HER stability test and the amount of oxygen increased distinctly according to the

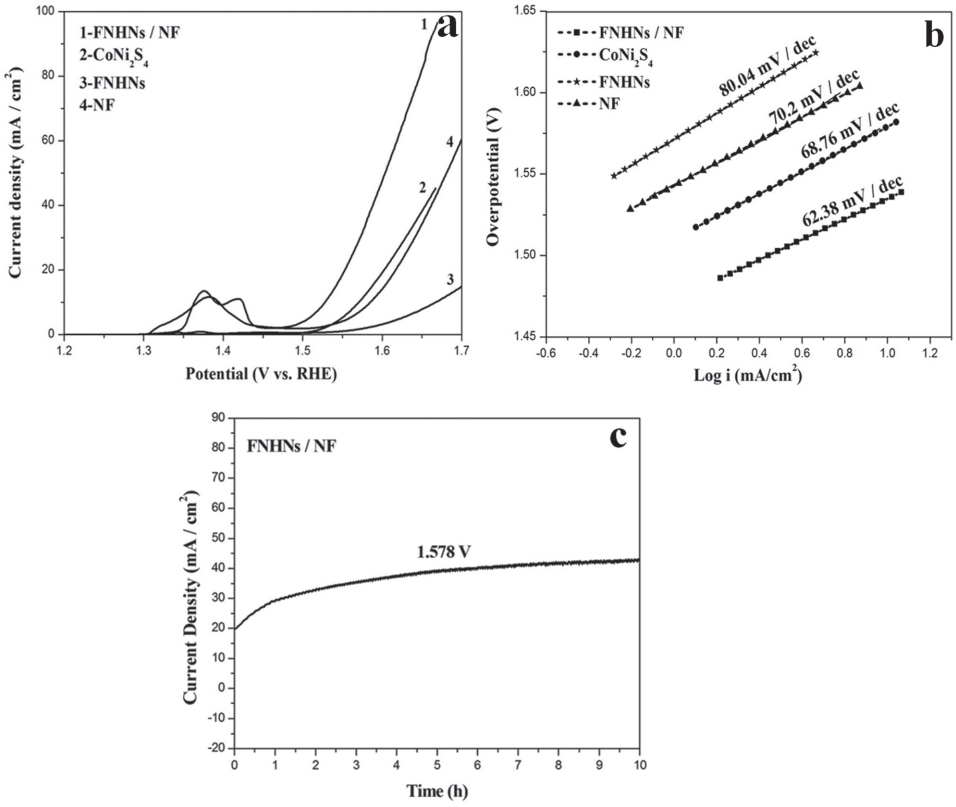

Figure 3. a) OER polarization curves (without iR-correction) of FNHNs/NF, $CoNi_2S_4$ FNHNs, FNHNs, and Ni foam with a scan rate of 1 mV s^{-1}. b) Corresponding Tafel plots of OER. c) The time-dependent current density curve of FNHNs/NF at a static potential of 1.578 V versus RHE for 10 h, in 1 M KOH.

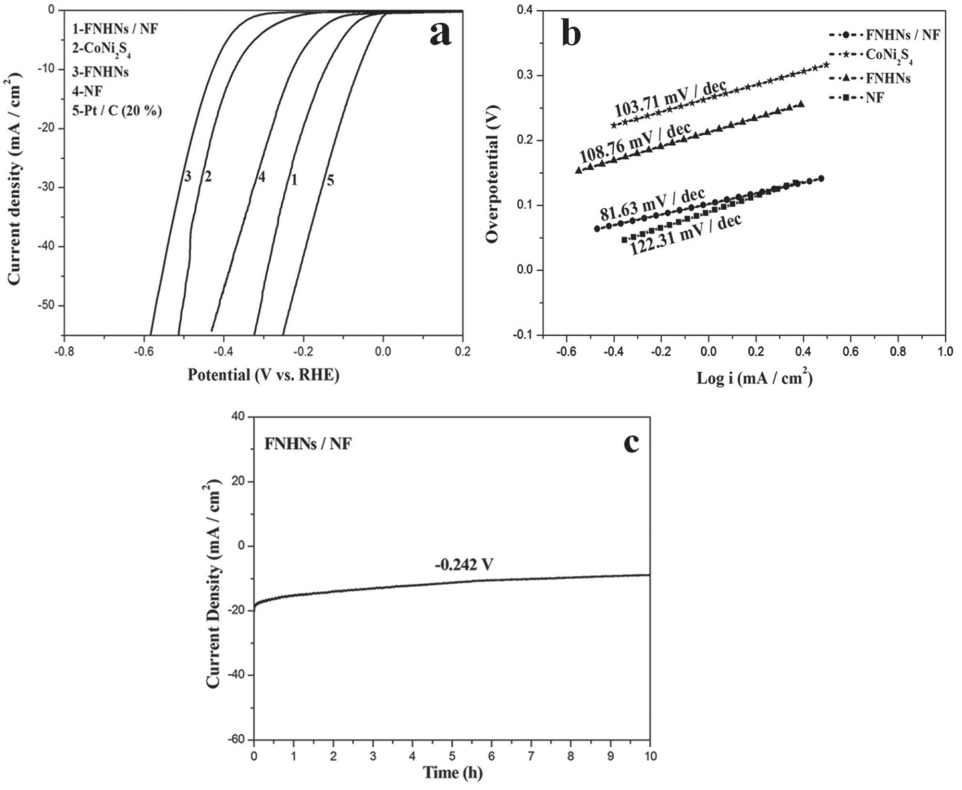

Figure 4. a) HER polarization curves (without iR-correction) of FNHNs/NF, $CoNi_2S_4$ FNHNs, FNHNs, Ni foam, and Pt/C (20%) with a scan rate of 1 mV s^{-1}. b) Corresponding Tafel plots of HER. c) The time-dependent current density curve of FNHNs/NF at a static potential of –0.242 V versus RHE for 10 h, in 1 M KOH.

element dispersion. Accordingly, it is reasonable for the current density to decrease during the process.

As a bifunctional catalyst, two pieces of FNHNs/NF (≈1 × 2 cm^2) were used to construct a two-electrode electrolyzer system. **Figure 5**a shows the simulated diagram, and the FNHNs (green spheres) disperse uniformly on the surface of NF. Figure 5b simulates a real overall water-splitting system in 1 M KOH solution. Apparently, there produced a lot of bubbles on the surfaces of anode and cathode continuously. Figure 5c displays the LSV plot of overall water splitting. It achieved 10 mA cm^{-2} at 1.55 V, which was much lower than some reported materials.[6] In a word, all of the experiments described above revealed that the FNHNs/NF is a highly effective bifunctional catalyst in strong alkaline electrolyte.

In summary, we have successfully synthesized in situ grown nickel oxysulfide fullerene-like hollow nanospheres on 3D nickel foams as a kind of efficient bifunctional electrocatalyst in strongly alkaline electrolytes (1 M KOH solution). Attributed to the extensive surface area, well conductive property of the nickel foam and the novel fullerene-like hollow nanospheres structure of nickel oxysulfide with uniform distribution and combination with the nickel foam closely, under the synergetic effect of FNHNs and nickel foam, the FNHNs/NF composite afford the current density of 10 mA cm^{-2} at low overpotentials of 0.29 V (vs RHE) for OER and 0.14 V for HER (vs RHE) in 1 M KOH. Furthermore, the FNHNs/NF could produce stable hydrogen and oxygen evolution at low overpotential over long period of time. Consequently, there is no doubt that the in situ growth of FNHNs on nickel foam by a solvothermal method would provide a promising direction for developing low-cost and high activity water-splitting electrocatalysts of non-noble metal oxysulfides.

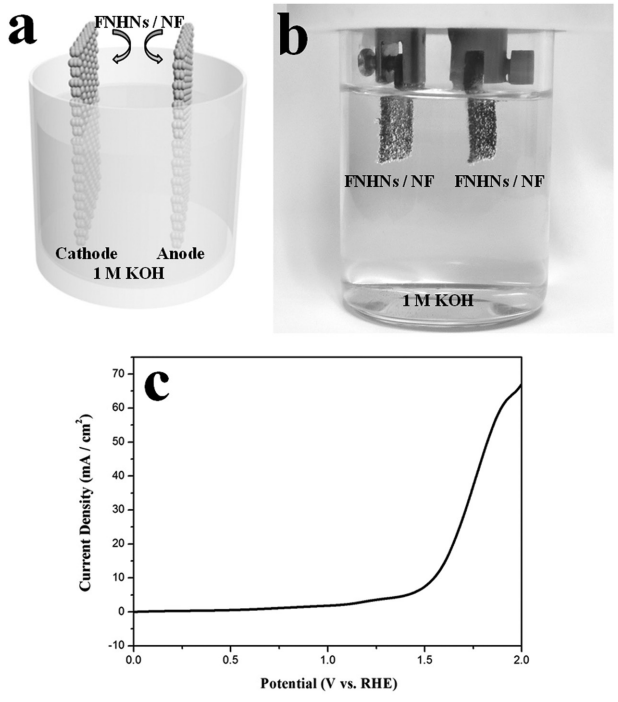

Figure 5. a) The simulated diagram of two-electrode electrolyzer system. b) The real image of two-electrode electrolyzer system (two pieces of FNHNs/NF (≈1 × 2 cm^2) as both the anode and cathode) with gas evolution in 1 M KOH solution. c) The linear sweep voltammetry (LSV) plot of overall water splitting by using FNHNs/NF as anode and cathode with the scan rate of 0.01 V s^{-1} in 1 M KOH.

Experimental Section

Materials: Nickel chloride hexahydrate ($NiCl_2{\cdot}6H_2O$), cobalt nitrate hexahydrate ($Co(NO_3)_2{\cdot}6H_2O$), S powder, oleic acid, and ethanol were purchased from Sinopharm Chemical Reagent Co., Ltd. *n*-Octylamine was bought from Aladdin Ltd. (Shanghai, China).

Characterization: TEM images were taken with a HITACHI H-7700. HRTEM (high resolution transmission electron microscopy) images, and energy-disperse X-ray spectra were taken with a Tecnai G2 F20 S-Twinhigh-resolution transmission electron microscope at 200 KV equipped with HAADF-STEM. SEM images were taken with a HITACHI SU8010. XRD characterization was carried on a BrukerD8 Advance using Cu Kα radiation (λ = 1.5418 Å). XPS were recorded on a PHI Quantera SXM spectrometer using monochromatic Al Kα X-ray sources (1486.6 eV). Electrochemical studies were carried out on a CHI660E B15057 electrochemistry workstation (CH Instruments, Inc., Shanghai). ICP-OES was measured on iCAP 6300 (ThermoFisher corporation).

Synthesis of Nickel Oxysulfide FNHNs: 0.0096 g S powder was weighed into 10 mL polytetrafluoroethene autoclave and 1 mL *n*-octylamine was added and stirred for 1 h. Then 2 mL oleic acid was injected into the autoclave. Finally the ethanol solution of $NiCl_2{\cdot}6H_2O$ (0.2377 g $NiCl_2{\cdot}6H_2O$ was dissolved in 6 mL ethanol) was transferred into the system and stirred for 30 min. After all these steps were done, the autoclave was sealed and put into oven set temperature at 180 °C for 8 h to react. After cooling down, the products were washed three times by using ethanol and centrifuged at 7000 rpm for 2 min. Then samples were dispersed in cyclohexane. The solution was diluted and a drop was dropped on TEM grid for morphology test.

The ratios of salts and solvent were optimized to get pure FNHNs. Changing them slightly could also get the FNHNs, but purity was lower.

Preparation of Nickel Oxysulfide/Ni Foam Composite: A piece of Ni foam (1 × 2 cm^2) was sonicated in acetone and 3 M HCl for 10 min respectively and sonicated in water and ethanol for several times. Subsequently, the dried nickel foam was immersed into the FNHNs reaction system (both the amount of reactants and operation procedure were same as above), which was then heated at 180 °C for 8 h. After rinsing with ethanol, the FNHNs/Ni foam composite was obtained.

Add Cobalt Salt to FNHNs System: 0.0085 g S powder was weighed into 10 mL polytetrafluoroethene autoclave and 0.8 mL *n*-octylamine was added to dissolve by stirring for 1 h. Then 1 mL oleic acid was injected into the autoclave. Finally the ethanol solution of $NiCl_2{\cdot}6H_2O$ (0.0951 g $NiCl_2{\cdot}6H_2O$ and a certain amount of $Co(NO_3)_2{\cdot}6H_2O$ were dissolved in 4 mL ethanol) was transferred into the system and stirred for 30 min. After all these steps were done, the autoclave was sealed and put into oven to react. Different ratios of $Co(NO_3)_2{\cdot}6H_2O$ were added to investigate the influence of other metal salts to the FNHNs system.

Electrochemical Measurements: In a typical sample preparation, the products were dried by vacuum drier at 30 °C for

several hours. Afterward, 5 mg products were dispersed in 1 mL cyclohexane and sonicated for 30 min. Then 6 µL dispersion were dropped on the glassy carbon electrode with a surface area of 0.196 cm^2. After the electrode surface was dried, 5 µL nafion @ ethanol (nafion: 0.5 wt%) was dropped on the surface of electrode. FNHNs/Ni foam composite (1×1 cm^2) was used to do electrochemical tests.

The OER and HER electrochemical performance were studied in a three-electrode configuration, in which graphite rod and Hg/Hg_2Cl_2 acted as the counter electrode and reference electrode, respectively. First, CV was used to stabilize and activate materials. When CV curves became stable, the rotation speed of electrode was set at 1600 rpm and the LSV was measured at scan rate of 5 mV s^{-1}. Subsequently, Tafel plots were obtained by taking advantage of the tafel plot function. Time-dependent current density curve was used to evaluate the electrocatalytic stability of materials.

Supporting Information

Supporting Information is available from the Wiley Online Library or from the author.

Acknowledgements

This work was supported by NSFC (21431003, 21521091) and China Ministry of Science and Technology under Contract of 2016YFA0202801.

[1] a) Y. Chen, R. Wu, P. Jiang, G. Bian, L. Kong, Y. Dong, *RSC Adv.* **2015**, *5*, 60674; b) N. Jiang, L. Bogoev, M. Popova, S. Gul, J. Yano, Y. Sun, *J. Mater. Chem. A* **2014**, *2*, 19407; c) J. Wang, W. Cui, Q. Liu, Z. Xing, A. M. Asiri, X. Sun, *Adv. Mater.* **2016**, *28*, 215.

[2] Q. Liu, J. Tian, W. Cui, P. Jiang, N. Cheng, A. M. Asiri, X. Sun, *Angew. Chem. Int. Ed.* **2014**, *53*, 6710.

[3] C. Tang, Z. Pu, Q. Liu, A. M. Asiri, Y. Luo, X. Sun, *Int. J. Hydro. Energy* **2015**, *40*, 4727.

[4] a) Q. Li, Z. Xing, A. M. Asiri, P. Jiang, X. Sun, *Int. J. Hydro. Energy* **2014**, *39*, 16806; b) Y. Tan, P. Liu, L. Chen, W. Cong, Y. Ito, J. Han, X. Guo, Z. Tang, T. Fujita, A. Hirata, M. W. Chen, *Adv. Mater.* **2014**, *26*, 8023.

[5] a) Y. R. Zheng, M. R. Gao, Q. Gao, H. H. Li, J. Xu, S. H. Yu, *Small* **2015**, *11*, 182; b) G. Song, J. Shen, F. Jiang, R. Hu, W. Li, L. An, R. Zou, Z. Chen, Z. Qin, J. Hu, *ACS Appl. Mater. Interfaces* **2014**, *6*, 3915.

[6] a) J. Luo, J.-H. Im, M. T. Mayer, M. Schreier, M. K. Nazeeruddin, N. G. Park, S. D. Tilley, H. Fan, M. Grätzel, *Science* **2014**, *345*, 1593; b) N. Jiang, B. You, M. Sheng, Y. Sun, *Angew. Chem., Int. Ed.* **2015**, *54*, 6251; c) W. Zhu, X. Yue, W. Zhang, S. Yu, Y. Zhang, J. Wang, J. Wang, *Chem. Commun.* **2016**, *52*, 1486; d) L. Feng, G. Yu, Y. Wu, G. Li, H. Li, Y. Sun, T. Asefa, W. Chen, X. Zou, *J. Am. Chem. Soc.* **2015**, *137*, 14023; e) D. Liu, Q. Lu, Y. Luo, X. Sun, A. M. Asiri, *Nanoscale* **2015**, *7*, 15122.

[7] a) J. I. Jung, H. Y. Jeong, J. S. Lee, M. G. Kim, J. Cho, *Angew. Chem. Int. Ed.* **2014**, *53*, 4582; b) B. Ni, X. Wang, *Chem. Sci.* **2015**, *6*, 3572; c) Y. Liu, G. D. Li, L. Yuan, L. Ge, H. Ding, D. Wang, X. Zou, *Nanoscale* **2015**, *7*, 3130; d) H. Wang, C. Tsai, D. Kong, K. Chan, F. Abild-Pedersen, J. K. Nørskov, Y. Cui, *Nano Res.* **2015**, *8*, 566; e) Y.-R. Zheng, M.-R. Gao, Z.-Y. Yu, Q. Gao, H.-L. Gao, S.-H. Yu, *Chem. Sci.* **2015**, *6*, 4594; f) H. Fei, J. Dong, M. J. Arellano-Jimenez, G. Ye, N. D. Kim, E. L. Samuel, Z. Peng, Z. Zhu, F. Qin, J. Bao, M. J. Yacaman, P. M. Ajayan, D. Chen, J. M. Tour, *Nat. Commun.* **2015**, *6*, 8668.

[8] a) Y. Yang, H. Fei, G. Ruan, C. Xiang, J. M. Tour, *Adv. Mater.* **2014**, *26*, 8163; b) C. Ouyang, X. Wang, S. Wang, *Chem. Commun.* **2015**, *51*, 14160; c) H. Ang, H. T. Tan, Z. M. Luo, Y. Zhang, Y. Y. Guo, G. Guo, H. Zhang, Q. Yan, *Small* **2015**, *11*, 6278; d) H. Wang, Z. Lu, S. Xu, D. Kong, J. J. Cha, G. Zheng, P. C. Hsu, K. Yan, D. Bradshaw, F. B. Prinz, Y. Cui, *Proc. Natl. Acad. Sci. USA* **2013**, *110*, 19701; e) H. Zhang, *ACS Nano* **2015**, *9*, 9451; f) M. Lukowski, A. Daniel, F. Meng, A. Forticaux, L. Li, S. Jin, *J. Am. Chem. Soc.* **2013**, *135*, 10274; g) M. Cabán-Acevedo, M. Stone, J. Schmidt, J. Thomas, Q. Ding, H. Chang, M. Tsai, J. He, S. Jin, *Nat. Mater.* **2015**, *14*, 1245; h) M. Faber, R. Dziedzic, M. Lukowski, N. S. Kaiser, Q. Ding, S. Jin, *J. Am. Chem. Soc.* **2014**, *136*, 10053; i) D. Kong, J. Cha, H. Wang, H. Leec, Y. Cui, *Energy Environ. Sci.* **2013**, *6*, 3553; j) H. Li, K. Yu, C. Li, Z. Tang, B. Guo, X. Lei, H. Fu, Z. Zhu, *Sci. Rep.* **2015**, *5*, 18730; k) J. Kibsgaard, Z. Chen, B. Reinecke, T. Jaramillo, *Nat. Mater.* **2012**, *11*, 963.

[9] J. Xu, J. Cui, C. Guo, Z. Zhao, R. Jiang, S. Xu, Z. Zhuang, Y. Huang, L. Wang, Y. Li, *Angew. Chem. Int. Ed.* **2016**, *55*, 6502.

[10] T.-W. Lin, C.-J. Liu, C.-S. Dai, *Appl. Catal. B* **2014**, *154–155*, 213.

[11] W. Zhou, X.-J. Wu, X. Cao, X. Huang, C. Tan, J. Tian, H. Liu, J. Wang, H. Zhang, *Energy Environ. Sci.* **2013**, *6*, 2921.

[12] K. Yan, Y. Lu, *Small* **2016**, *12*, 2975.

[13] F. Song, X. Hu, *Nat. Commun.* **2014**, *5*, 4477.

[14] W. Zhou, X. Wu, X. Cao, X. Huang, C. Tan, J. Tian, H. Liu, J. Wang, H. Zhang, *Energy Environ. Sci.* **2013**, *6*, 2921.

[15] a) L. Han, X. Y. Yu, X. W. Lou, *Adv. Mater.* **2016**, *28*, 4601; b) C. T. Cherian, M. V. Reddy, S. C. Haur, B. V. Chowdari, *ACS Appl. Mater. Interfaces* **2013**, *5*, 918; c) S. Peng, L. Li, X. Han, W. Sun, M. Srinivasan, S. G. Mhaisalkar, F. Cheng, Q. Yan, J. Chen, S. Ramakrishna, *Angew. Chem. Int. Ed.* **2014**, *53*, 12594; d) N. Jiang, B. You, M. Sheng, Y. Sun, *Angew. Chem. Int. Ed.* **2015**, *54*, 6251.

[16] J. Zhang, T. Wang, D. Pohl, B. Rellinghaus, R. Dong, S. Liu, X. Zhuang, X. Feng, *Angew. Chem. Int. Ed.* **2016**, *55*, 6702.

[17] Y. Zhao, B. Sun, X. Huang, H. Liu, D. Su, K. Sun, G. Wang, *J. Mater. Chem. A* **2015**, *3*, 5402.

Received: August 9, 2016
Revised: October 16, 2016
Published online: November 18, 2016

